Extracting Optimal Preparation Parameters of TiO2 Electron Transmission Layer in Perovskite Solar Cell for Increasing Efficiency of the Cell

Ghahraman Solookinejad (ghsolooki@gmail.com)
Islamic Azad University Marvdasht https://orcid.org/0000-0002-5521-0190
Mohsen Vaezzadeh Asadi
Islamic Azad University Marvdasht
Heydar Izadneshan
Islamic Azad University Marvdasht

Research

Keywords: titanium dioxide, Radio

Posted Date: November 18th, 2020

DOI: https://doi.org/10.21203/rs.3.rs-87980/v1

Extracting optimal preparation parameters of TiO_2 electron transmission layer in perovskite solar cell for increasing efficiency of the cell

Ghahraman Solookinejad[1*], Mohsen. Vaezzadeh Asadi[1] and Heydar. Izadneshan[1]

Abstract

In this research, a thin film of titanium dioxide was prepared as electron transporting layer to be used in perovskite solar cell simulation. The thin film TiO_2 was prepared under different lab conditions such as changing the chamber pressure from 2.0×10^{-2} to 4.0×10^{-2} mbar and changing the power of deposition device from 200 to 240 watts for different thickness ranging from 30 to 150 nm. Radio frequency magnetron sputtering method has been used to fabricate the layers under the mentioned laboratory conditions. Then, the band gap energy of the thin films was calculated by Tauc's plot method. It was shown that the bands gap energy which is one of the contributing factors in solar cell characteristics, such as short-circuit current, open-circuit voltage, fill factor and solar cell efficiency, highly depends on laboratory conditions of preparing the thin film and it changes with changes in deposition parameters of the device. The simulated solar cells were considered as ZnO: Al / TiO_2 compact layer/ $CH_3NH_3SnI_3$ / CuI / Au. Investigation on the effects of preparation conditions of TiO_2 on properties of the cell and perovskite solar efficiency was carried out using experimental data related to TiO_2 and extraction of data of other layers from authentic articles using comsol multiphysics software. In comparison with other preparation conditions, the prepared layer with 30 nm thickness under 240 watts device power and 3.5×10^{-2} mbar chamber pressure had the best possible results. In this condition, perovskite solar cell characteristics obtained I_{sc} = 22.368mA, V_{oc} = 1.02V, % FF = 80.522 and % PCE = 18.371.

Introduction

Economic crises and other problems like fossil fuels decline and their destructive effects on the environment as well as the rise of energy consumption due to world population increase [1] have made scientists to find appropriate solutions to solve global energy and its environmental impact problem [2, 3]. Developed countries and developing countries are using renewable energy sources like sunlight, wind, water, etc. to provide clean energy sources and consequently decrease detrimental environmental hazards, greenhouse gasses, and global warming [4]. The only solution to these problems is to use renewable energy sources. Nowadays, the strategy of the world's countries is to use renewable energies especially solar photovoltaic energy [5]. Solar energy is one of the renewable sources; this endless energy source has the potential to solve most of the mentioned problems [6]. Solar cells can solve human's energy needs by receiving sunlight and converting it into electrical energy. This energy can be used in different industries. The naming of different solar cells is based on their semi-conductor materials. These materials should have specific characteristics to absorb the sunlight. Some kinds of solar cells have been made of different compounds like silicon solar cells [7], cadmium-telluride [8], gallium arsenide [9], hybrid solar cells composed of semi-conductor organic a non - organic materials [10], bio-hybrid solar cells [11, 12], and recently perovskite solar cells [13] that is the purpose of this article. Inclusion of lead as a feature of perovskite material is a common concern. Tin-based perovskite absorbents like $CH_3NH_3SnI_3$ have been reported with lower power efficiency [14, 15]. In their structure, generally, solar cells have that they have been made of different layers to convert luminous energy to electrical energy. Semi-conductor nano-materials are promising options for the economic and environment friendly system having copious chemical and catalyst non-toxic energy sources without any secondary pollution.

There are many semi-conductor compounds which can be used as anti-reflection coating in solar cells, the most important of them are Sio_2 [16], ZnS [17], MgF2 [18], ZnO [19], and Tio_2 [19]. Titanium dioxide is one the most highly used anti-reflection materials. Its natural stability is titanium oxide [20]. Titanium dioxide can be prepared in three main phases of brookite, anatase, and rutile [21]. This material has a wide range of application in the paint industry, paper industry, plastic, glaze, glass industry, cosmetic products, water refinery (as catalyst) [22, 23], isolators, sensors, etc. Titanium dioxide is the most appropriate candidate to be used in solar cells due to having peculiar physical-chemical properties such as high stability in the vast environment around in high acidity [24], high refractive index [25, 26] and the very low edge of conduction band to energy balances of light absorbent layers [27]. In general, titanium dioxide is used as electron transporting layer in solar cells. For instance, since the conduction edge of titanium dioxide in solar cells sensitive

* Correspondence: ghsolooki@gmail.com

[1]Department of physics, Islamic Azad University, marvdasht Branch, Marvdasht, Iran

to pigment is a little bit smaller than the energy of excited state of most of the sensitive pigments, an electron can be injected efficiently. Moreover, having high refractive index, titanium dioxide prevents recombination before reproduction by an oxidative electrolyte [28]. This material is a good candidate for using solar cells. Because of its high refractive index [29], titanium dioxide can be used as a white pigment or transparency regulator in powder form [30]. Recently, it has been shown that, to increase light trapping capacity in perovskite solar cells, TiO_2 can be prepared in form of nano-tube or nano-particles [31] or nano-bar and nano-particle through the hydrothermal method. It's been shown that perovskite solar cell efficiency obtained 12.2% [32]. Currently, photovoltaic cells with heterojunctions are being seriously investigated because they are a promising route toward converting solar energy with high efficiency and low cost [33-36]. There has been considerable growth in the development of perovskite solar cells since 2008 [37]. The efficiency of perovskite solar cell increased from 3.1% in 2009 to 3.8% in 2011 [38], 6.5% in 2012 [39] to 9.7% [40] and 10.9% [41]. Then, with relatively rapid growth, the efficiency reached to 15.3% in 2013 [42, 43]. In 2015, the chemical technology research institute of South Korea (KRICT) reported the efficiency of solid-state perovskite solar cells 17.9%. More recently, perovskite solar cell efficiency has enhanced approximately to 22.1% [44, 45] for a cell with a cross-sectional area less than 0.1cm2. This study investigated. the effect of lab conditions on preparation of titanium dioxide layer as one of the most highly used layers in different solar cells especially perovskite. This layer was prepared experimentally under different lab conditions like chamber pressure change and device power change using radio frequency magnetron sputtering method. Then, the effect of lab conditions on preparation of titanium dioxide layer on perovskite solar cell parameters such as short-circuit current, open-circuit voltage, fill factor, and solar cell efficiency was investigated. Thus, the required information of other layers was selected from valid sources, then simulation was performed using comsol multiphysics software.

Materials and methods

This study used radio frequency magnetron sputtering device model MSS – MDAU 160 from an injection of Argon neutral gas with 99.99% purity. Titanium dioxide tablet had a thickness of 3 mm, a diameter of 76.2 mm and purity of 99.99%. The fixed value of 5 cm was selected as the target distance to substrate for deposition. The normal glass substrate of (2 cm × 5 cm) was used for deposition. In this research, the effects of lab conditions of the preparation of titanium dioxide for different thicknesses in fixed deposition pressure and power as well as a fixed thickness under different deposition pressure and power are examined using radio frequency magnetron sputtering method.

Sample preparation

Lab conditions and deposition process

First, all substrates were washed with distilled water for 15 minutes. Then, the substrates were washed several times with acetone and placed in alcohol for 10 minutes to remove all impurities. Before starting the main deposition on substrates, to purify the vacuum chamber, the initial pressure inside the chamber was reached to 3.0×10^{-5} mbar to minimize the pollution inside the environment. After adjusting the device and formation of plasma for deposition, a deposition was carried out tentatively for 10 minutes to remove all possible impurities on the target tablet. After these stages and ensuring the minimization of the chamber pollution and substrate, a plasma was formed for deposition by regulating the initial power of 500 watts and a chamber pressure of 3.0×10^{-5}mbar and deposition of different lab conditions was completed. During the deposition process, the temperature inside the chamber was kept fixed for 58^0C. Then, using Argon gas, five thicknesses of 30, 75, 60, 90, 105 nm were deposited with power 240 watts and 3.5×10^{-2} mbar chamber pressure as shown in the table (1). In the next step, by selecting the fixed thickness of 30 nm, this thickness was deposited once with the fixed 220 watts power under different pressures inside the chamber as shown in the table (2).

The next time, the chamber pressure kept fixed 3.5×10-2 mbar and deposition were carried out with different powers as shown in the table (3). Then, to specify coefficient absorption and using it determine bands gap energy, the layers were lighted by Perkins Elmer model Lambda 45. A sample of a substrate without coating was placed in the device and its absorption rate became zero for further accurate measurements of substrates with coating. Lighting the prepared layers was completed in wavelength of the visible light spectrum of (320-900) nm. Laboratory samples made are shown in figure (1).

Fig 1 Tio2 laboratory samples made in different laboratory conditions.

Table 1 Deposition under fixed power& pressure of device for different thicknesses

Table 2 Deposition under fixed power of device for fixed thicknesses 30 nm under different chamber pressure.

Table 3 Deposition under fixed chamber pressure for 30 nm layer under different powers of device

.

Characterization

Determining band gap energy

There are different methods such as Beer-Lambert law [46] and Tauc's plot [47] for calculating bands gap energy. This research used Tauc's plot method for measuring bands gap energy. Coefficient absorption (equation 1) can be described based on a function of Photon energy (eV) and used to calculate bands gap energy:

$$\alpha h\nu = A\,(Eg - h\nu)^{n} \quad (1)$$

Where fixed h is Planck's constant, ν is frequency, n is the numerical value which is dependent on transition nature having values of 1/2, 2, and 3/2 for direct, indirect and forbidden transition. Regarding that Tio_2 is a semi-conductor or direct band gap transition, the value of 1/2 was considered for n [48]. Therefore, with drawing $(\alpha h\nu)^2$ versus hν and extrapolation of the linear area of the curve in α=0, direct bands gap energy for titanium dioxide is calculated.

Fig. 2 Tauc's plot for the thin film prepared TiO_2 a) different thicknesses, b) under different pressures, c) Different powers

The final results of extraction of bands gap energy of the prepared layers under different conditions using figures (2- a, 2-b and 2-c) are shown in table (4).

Table 4 The extracted band gap energy related to Tio2 compact layer.

Methodology

Computational simulation is a method of studying and analyzing the behavior of a real device by a hypothetical system using a computer program. Simulation is based on a mathematical model that describes the system. For years, it's been confirmed that numerical simulation method of solar cell device is a valid instrument for studying and understanding properties of solar cell devices like optical, electrical and mechanical properties [49]. Numerical simulation has been used for studying the performance of the solar cell for 40 years [50]. With development of these numerical models, a clear understanding of the mechanism of solar cells has been obtained which has led considerably to improvement and development of the performance and efficiency of the device. Comsol multiphysics software is a complete set of simulation which can solve differential equations of non-linear systems by partial derivatives through FEM method in one, two, and three-dimensional space. This is a numerical method for approximate solution of partial differential equations using numerical methods like Euler method. Comsol multiphysics software can examine thin film systems and photonic structures properly. This study designs and investigates tin-based perovskite solar cell efficiency using experimental results and previous studies simultaneously through simulation in comsol multiphysics software.

Device structure

According to figure (3), tin-based perovskite solar cell is considered as flat heterojunction, TiO_2 is the electron transporting material, $CH_3NH_3SnI_3$ is the absorbent layer and CuI is hole transporting material. ZnO: Al and Au are the front and back contact respectively.

Fig. 3 a) Schematic structure and b) perovskite solar cell energy diagram $CH_3NH_3SnI_3$

The parameters used in simulation

The parameters used in simulation of different layers were meticulously selected from experimental data of this study and previous studies. The data related to TiO_2 like different thicknesses and bands gap energy measured under deposition conditions in the first section of this study were entered into the simulation. Table (5) shows the simulation parameters.

Table 5 The selected parameters for simulation process in AM1.5G.

In this simulation, the recombination process was considered Shockley-Reed-Hall recombination [60] and doped impurities assumed 10^{17} (1/cm3). After the completion of simulation and extraction of data from I-V curve using $FF=(Imp \times V_{mp})/(I_{sc} \times V_{oc})$ and $PCE = (FF \times I_{sc} \times V_{oc})/P_{in}$ where Imp and V_{mp} are voltage and current in maximum power and I_{sc} and V_{oc} are open-circuit voltage and short-circuit voltage and P_{in} is the power of the incident light to solar cell surface, the fill factor and perovskite solar cell efficiency can be calculated. The cross section of the perovskite solar cell is considered to be $2cm^2$ and comsol multiphysics software considers the connection model to be an ideal ohmic and the ideal ohmic connection equation have been used [61]. Graphs are down using MATLAB Software. The I-V curves were extracted by combining the data related to prepare TiO_2 layer under different physical conditions experimentally and the data of table (4) in comsol multiphysics software. Using these

diagrams, I_{sc}, V_{oc} ،% FF and % PCE of perovskite solar cell for all three states can be obtained.

Different thicknesses of the prepared layers under fixed power and pressure

I-V curves and perovskite solar cell parameters for different thicknesses are shown in the figure (4) and table (6), respectively.

Fig. 4 I-V curve perovskite solar cell for different thicknesses.

Table 6 Perovskite solar cell parameters for different thicknesses

The prepared layers TiO_2 with 30nm thickness under fixed power and different pressures of chamber

As can be seen from figure (4), the I-V diagram is quite sensitive to changes in the thickness of the Tio_2 layer. As the thickness increases, the short-circuit current decreases. But there is no change in the open-circuit voltage. I-V curves and perovskite solar cell parameters for 30 nm thickness under different pressures of chamber are shown in figure (5) and table (7), respectively.

Fig. 5 I-V curve perovskite solar cell for different pressures.

Table 7. Perovskite solar cell parameters for different pressures

Figure (5) shows an overlap for the simulated I-V diagrams. The figure (5-a), (from a close-up view) shows that under the mentioned conditions, the numerical values of short-circuit currents (table 7) are very close to each other. That is, the pressure change in the preparation of the Tio_2 layer has very little effect on the short-circuit current. The figure (5-b) shows that no change in open-circuit voltage is observed.

The prepared layers TiO_2 with 30nm thickness under the fixed pressure and different powers device

I-V curves and perovskite solar cell parameters for 30 nm thickness under different powers of chamber are shown in figure (6) and table (8), respectively.

Fig. 6 I-V curve perovskite solar cell for different powers.

Table 8 Perovskite solar cell parameters for different powers

Figure (6) shows that as the power of the device increases from 200 to 220 watts, an increase in short-circuit current occurs. Then, by increasing the power of the device from 220 to 240 watts, the open-circuit current increases by 0.004mA compared to the power of 220 watts (table 8), which is not considered a significant change. In other words, an overlap has occurred as shown in Figure (6- a). Figure (6-b) shows that as the power of the device changes, the open- circuit voltage remains constant and does not depend on the change in power of the device.

Results and Discussion

The effect of thickness on the band gap energy of TiO_2 prepared at constant pressure and power

Table (4) shows the change of bands gap energy versus the drawn thickness and the effect of thickness on bands gap energy as shown in figure (7).

Fig. 7 TiO2 compact layer bands gap energy as a function of the layer's thickness.

The dependence of photovoltaic performance on thickness of the TiO_2 thin film

Figure (8-a) shows that I_{sc} significantly depends on the change of the thin film thickness and it decreases with the increase of thickness. In 30 to 105 nm range, I_{sc} changes from 22.37(mA) to 19.64(mA) and the current declines 12% approximately.

This behavior can be explained in this way: there are two ways for transporting charge from perovskite to side current, one of them via TiO_2 and the other one via perovskite itself [62, 63]. In structures having an approximate thickness of 1 µm (like the selected structure in this article), regarding the lower conduction band of TiO_2 in comparison to lower perovskite's unoccupied molecular orbital, the rate of TiO_2 is much lower than perovskite electron transport. Therefore, the capacity of electron transport from compact layer shows higher dependence on thickness [63, 64] and the other reason can be related to increase of thickness so that pair electron - hole are produced and recombined before reaching the contacts. V_{oc} decreased slightly with an increase of thickness which can be disregarded. In other words, V_{oc} is to some extent independent of the compact layer thickness [64] With the change of I_{sc}, fill factor and consequently the perovskite solar cell TiO_2 acts as an anti-reflector layer in solar cells and transparency of TiO_2 thin film is of paramount importance. This layer should be as thin as possible to decline its

resistance against the current. The thickness of the layer allows more light to pass and reach a perovskite absorbent layer for production of the pair electron-hole. The series resistance is proportionate to a thickness so that the less the thickness the less the series resistance and the more the current. The increase of the thickness increases the TiO_2 layer's series resistance which thin film is of paramount importance. This layer should be as thin as possible to decline its resistance against the current. The thickness of the layer allows more light to pass and reach a perovskite absorbent layer for production of the pair electron-hole. The series resistance is proportionate to a thickness so that the less the thickness the less the series resistance and the more the current. The increase of the thickness increases the TiO_2 layer's series resistance which leads to a decrease in I_{sc} current and decreases the efficiency in consequence. The electron transporting layer impacts on the performance of solar cell: the resistance should be low as much as possible and the thickness should be as thin as possible. Therefore, to transport the electron and the hole, the edge of conduction band of TiO_2 should be under perovskite's conduction band and its valance should be under perovskite's valance band. According to figure (8-b), V_{oc} has not changed, (1.02), which it can be concluded that during shining the rate of production and recombination of electrons and holes almost remains fixed and V_{oc} does not change as a result. In addition to the mentioned factors, there is a peculiar relationship between V_{oc} and contributing factors including energetic disorder, charge transfer states, donor-acceptor interface, micro-structure, carrier density, etc. Each of which having a special importance in V_{oc}. Other parameters like electrode work function, morphology, light intensity, density of state (DOS) recombination, temperature, and defect state and crystallinity impact on open-circuit voltage of organic solar cells with heterogeneous junction directly or indirectly. The amount on the effect of each of these factors can be considered separately [65]. According to figures (8-a) and (8-b), the rate of efficiency solar cell (% PCE) as shown in figure (8-d), change is similar to I_{sc} showing that the efficiency is all dependent on short current circuit. It should be noted that the change of fill factor as shown in figure (8-c) needs more investigations. The fill factor depends on the short-circuit current and the open-circuit voltage. For example, open-circuit voltage depends on various factors such as morphology, electrodes work function, light intensity, recombination and etc. [64]. In this paper, only the effect of physical conditions on the fabrication of the titanium dioxide layer is investigated. Therefore, the effect of other factors on the fill factor should be investigated, which requires more investigations.

Fig. 8 Compact layer (CL) thickness-dependent variation in (a) Is c, (b) Vo c, (c) % FF, and (d) % PCE.

The effect of pressure on the band gap energy of TiO_2 prepared at constant thickness and power

Using table (4), the change of bands gap energy versus different chamber pressures is drawn and the effect of pressure on bands gap energy is shown in figure 9.

Fig 9 TiO_2 compact layer bands gap energy as a function of chamber's pressure.

The dependence of photovoltaic performance on construction of TiO_2 thin film in different pressures

Figure (10-a) shows that $I_{s\,c}$ depends slightly on the change of chamber's pressure in making of the thin film so that with the increase of the chamber pressure from 0.02 to 0.04 mbar, it changes and increases from 22.356 mA to 22.364 mA. In other words, with the increase of the chamber pressure, a slight increase about 0.04% happens which can be disregarded and it can be said that I_{sc} is almost independent of the chamber pressure during the layer making. The approximate fixed state of short-circuit current means that the series resistance is almost fixed under different conditions of the layer making and the capacity of electron transport of this layer has almost not changed. In general, V_{oc} is resulted from the splitting of quasi-fermi levels and the hole caused by shining.

$$V_{oc} = 1/q\,(E_{FN} - E_{FP}) \qquad (2)$$

Where q is elementary charge and E_{FN} and E_{FP} are respectively electron and hole quasi-fermi energy levels [65]. Under open-circuit conditions, when switching off the source of light shining, the charge carriers caused by light are not produced, and naturally due to recombination phenomenon, the number of electrons and holes decreases and V_{oc} declines theoretically [66]. Regarding that V_{oc} remains fixed, (1.02), according to figure (10-b), it can be concluded that during shining the rate of production and recombination of electrons and holes almost remains fixed and V_{oc} does not change as a result. Regarding the reliance of FF as shown in figure (10-c), on short-circuit current and open-circuit voltage and fixity of I_{sc} and V_{oc}, this parameter also remained fixed. Regarding the reliance of solar cell efficiency on I_{sc}, V_{oc} and FF, the efficiency changes with the change in $I_{s\,c}$, V_{oc} and % FF. Since V_{oc} and FF are fixed and independent of the chamber pressure, as shown in figure (10-a) and (10-b), it is all clear that the solar cell efficiency (% PCE) as shown in figure (10-d), has changed slightly with I_{sc} change. Since the change is very subtle. This means that according to table 8, this change is something around 0.038%, which is very small.

It can be concluded that efficiency of the simulated perovskite solar cell is almost independent of the changes in chamber's pressure in making of compact layer of titanium dioxide.

Fig. 10 Compact layer (CL) pressure-dependent variation in a) Isc, b) Voc, c) % FF, and d) % PCE

The effect of device deposition power on the band gap energy of TiO_2 prepared at constant thickness and pressure

Parameters Using table (4), the change of bands gap energy versus different deposition powers are drawn and the effect of bands gap energy power is shown in figure 11.

Fig. 11 TiO_2 compact layer bands gap energy as a function of deposition power.

According to table (4) and figure (7, 9 and 11), the rate of bands gap change is (3.618 to 3.687) eV, which shows that bands gap energy highly depends on the conditions under which the process is carried out [67]. Titanium dioxide's bands gap energy deposited through DC magnetron sputtering method under different powers and pressures in (3.20-3.28) eV limit which is in line with the results of this study [68]. The bands gap energy of thin film of titanium dioxide with mixed phase has been reported in (3.58 to 3.75) eV limit [69] which is in line with bands gap energy of this study in (3.576-3.687) eV.

The dependence of photovoltaic performance on TiO_2 thin film in different deposition power

Figure (12-a) shows that I_{sc} depends on the change of deposition power of the device and with an increase of the power, in 200 to 240 watts, I_{sc} current changes from 14.899(mA) to 22.368 (mA) and an approximate current increase of 33% happens. In other words, the series resistance decreases with the increase of the power and the current increases as a consequence. According to figure (12-b), V_{oc} remain fixed, (1.02), showing that the change in deposition power has no effect on the open-circuit voltage. Regarding the fixity of V_{oc}, the change trend of % FF as shown in figure (12-c), has an ascending pattern with an increase of power. With the reliance of this parameter on I_{sc}, its change trend is almost proportionate to short-circuit current having an ascending trend with an increase of power. Finally, the efficiency of perovskite solar cell (% PCE) as shown in figure (12-d) increases with power increase so that it reaches to its highest rate of 18.371% in 240 watts.

Fig. 12 compact layer (CL) Power-dependent variation in a) Isc, b) Voc, c) % FF, and d) % PCE

Conclusion

The simulation technique of a solar cell for investigating its parameters like I_{sc}, V_{oc}, % FF, % PCE is very useful and low cost. In this study, thin layer of TiO_2 was prepared under different lab conditions like thickness, changing deposition power of the device and changing chamber pressure using radio frequency magnetron sputtering method and its effects on optical parameters of bands gap energy of TiO_2 thin layer was investigated. In the next step, a tin-based perovskite solar cell was simulated by COMSOL multiphysics software followed by analysis of the effect of the preparation conditions of TiO_2 electron transporting layer on the performance and efficiency of the solar cell. The tin-based perovskite solar cell is important since tin is not toxic and is easily accessible with low cost. The results of the simulation showed that the 30 nm layer under 240 watts power and 3.5×10^{-2} mbar pressure was the most appropriate layer for trapping light. In this prepared layer, the highest efficiency was % PCE = 18.371 and other parameters obtained I_{sc} = 22.368 mA, V_{oc} = 1.02mV, % FF = 80.522.

Declaration of competing interest

1.Availability of data and materials (not applicable) and the reason is the disagreement of all the authors of the article.
2.The author(s) declare(s) that they have no known competing financial interests.
3. funding (not applicable)
4.authors' contributions (Ghahraman Solookinejad (corresponding author) and Mohsen Vaezzadeh Asadi and Heydar Izadneshan are Co-authors).
5.Acknowledgements from labs of Physics and Chemistry Departments of Islamic Azad University Marvdasht and the developers of COMSOL Multiphysics Software.
6.Personal relationships (not applicable).
7.Authors' information that could have appeared to influence the work reported in this paper.

Acknowledgements

The author of the article appreciates the helps and cooperation of thin layer and analytical chemistry labs of Physics and Chemistry Departments of Islamic Azad University Marvdasht for preparing and spectroscopy of UV-VIS of the thin layer of TiO_2. The author also deeply thanks to the developers of COMSOL Multiphysics software.

References

1. Kulkarni, S.H., Anil, T.R.: Rural Electrification through Renewable Energy Sources- An Overview of Challenges and Prospects. International Journal of Engineering Research. 3, 384 (2014)
2. Stone, J.L.: unlimited electrical energy from the sun. Physics Today. 2780, 1990 (1999)
3. Stone, J.L.: unlimited electrical energy from the sun. Photovoltaics. 4, 9 (1993)
4. Herzog, A.V, Lipman, T.E., Kammen, D.M.: Perspective and Overview of Life Support systems and Sustainable Development Perspective and Overview of Life Support systems and Sustainable Development, (University of California, Berkeley), 2001.
5. Sommerfeld, J., Buys, I., Vine, D.: Residential consumers' experiences in the adoption and use of solar PV. Energy Policy. 105, 10 (2017)
6. Lior, N.: Sustainable energy development: The present (2009) situation and possible paths to the future Energy. 35, 3976 (2010)

7. Heywang, W., Zaininger, K.H.: Silicon: the semiconductor material, in Silicon: evolution and future of a technology evolution and future of a technology, (Springer Verlag) (2004)

8. Fthenakis, V., Kim, H.C.: Life-cycle uses of water in U.S. electricity generation Renewable and Sustainable Energy Reviews. 14, 2039 (2010)

9. Moss, S.J., Ledwith, A.: The Chemistry of the Semiconductor Industry. (Springer) (1987)

10. Milliron, D.J., Gur, I., Alivisatos, A.P.: Hybrid Organic–Nanocrystal Solar Cells MRS Bulletin. 30, 41 (2005)

11. Ciesielskia, P.N., Hijazib, F.M., Scott, A. M., Faulkner, Ch.J., Beard, L. Emmett, K., Rosenthal, S.J., Cliffel, D., Kane Jennings, G.: photosystem I- Based biohybrid phtoelectrochemical cells. Biosource Technology, 101, 3047 (2013)

12. Omer, Y., Tel-Vered, R., Wasserman, J., Trifonov, A. Michaeli, D. Nechushtai, R., Willner, I.: Integrated photosytem II Based photoelectrochemical cells Nature communication. 3, (2012)

13. Eperon, G.E., Stranks, S.D., Menelaou, Ch., Johnston, M.B., Herz, L.M., Snaith, H.J.: Formamidinium lead trihalide: a broadly tunable perovskite for efficient planar heterojunction solar cells Energy & Environmental Science. 7, 982 (2014)

14. Noel, N.K., Stranks, S.D., Abate, A., Wehrenfennig, Ch., Guarnera, S., Haghighirad, A., Sadhanala, A., Eperon, G.E., Pathak, S.K., Johnston, M.B., Petrozza, A., Herz, L.M., Snaith, H.J.: Lead-free organic–inorganic tin halide perovskites for photovoltaic applications. Energy & Environmental Science. 7, 3061 (2014)

15. Askari, M.B., Mirzaei Mahmoud Abadi, V., Mirhabibi, M.: Types of Solar Cells and Application American Journal of Optics and Photonics. 3, 94 (2015)

16. Ali, Kh., Khan, S.A., Mat Jafri, M.Z.: Effect of Double Layer (SiO2/TiO2) Anti-reflective Coating on Silicon Solar Cells. Int. J. Electrochem. Sci. 9, 7865 (2014)

17. Salih, A.T., Najim, A.A., Muhi, M.A.H., Gbashi, K.R.: Single-material multilayer ZnS as anti-reflective coating for solar cell applications. Optics Communications. 388, 84 (2017)

18. Karthik, D., Pendse, S., Sakthivel, Sh., Ramasamy, E., Joshi, Sh.V.: High performance broad band antireflective coatings using a facile synthesis of ink-bottle mesoporous MgF2 nanoparticles for solar applications. Solar Energy Materials and Solar Cells. 159, 204 (2017)

19. Ulbrich, C., Gerber, A., Hermans, K., Lambertz, A., Rau, U.: Analysis of short circuit current gains by an anti-reflective textured cover on silicon thin film solar cells. Progress in photovoltaics. 21, 1672 (2013)

20. Max Planck institute for solid state research. (2016)

21. Zabon, A., Aruna, S.T., Tirosh, S., Gregg, B.A., Mastai, Y.: The effect of the preparations condition of TiO2 colloids on their surface structures. J. Phys. Chem. B. 104, 4130 (2000)

22. Cai, Q., Hu, J.: Effect of UVA/LED/TiO_2 photocatalysis treated sulfamethoxazole and trimethoprim containing wastewater on antibiotic resistance development in sequencing batch reactors. Water Res. 140, 251 (2018)

23. Pouretedal, H.R.: Visible photocatalytic activity of co-dapted TiO_2/Zr, N nanoparticles in wastewater treatment of nitrotoluene sample. J. Alloys. Compd. 735, 2507 (2018)

24. Allen, N.S., Edge, M., Ortega, A., liauw, C., Stratton, J., McIntyre R.B.: Behaviour of nanoparticle (ultrafine) titanium dioxide pigments and stabilisers on the photooxidative stability of water based acrylic and isocyanate based acrylic coatings. Polymer Degradation and Stability. 78, 467 (2002)

25. Flaim, T., Wang, Y., Mercado R.: High Refractive Index Polymer Coatings for Optoelectronics Applications. Proceedings of SPIE - The International Society for Optical Engineering. (2004)

26. An, N. Wang, K., Wei, H., Song, Q. Xiao, Sh.: Fabricating high refractive index titanium dioxide film using electron beam evaporation for all-dielectric metasurfaces. MRS Communications, 1 (2016)

27. Murakami, T.N., Miyadera, T., Funaki, T., Cojokaro, L., Kazaoui, S., Chikamatsu, M., Segawa, H.: Adjustment of conduction band edge of compact TiO_2 layer in perovskite solar cells through $TiCl_4$ treatment. ACS Appl. Mater. Interfaces. 9, 36708 (2017)

28. Hagfeldt, A., Boschloo, G., Sun, L., Kloo, L., Pettersson, H.: Dye-sensitized solar cells. Chem. Rev. 110, 6595 (2010)

29. Siefke, T., Kroker, S., Pfeiffer, K., Puffky, O., Dietrich, K., Franta, D., Ohlídal, I., Szeghalmi, A., Kley, E.-B., Tünnermann, A.: Materials pushing the application limits of wire grid polarizers further into the deep ultraviolet spectral range. Adv. optical Maters. 4, 1780 (2016)

30. Krebs, R.E.: The History and use of our Earths Chemical Elements, (Green Wood Press) (2006)

31. Yang, H.-Y., Rho, W.-Y., Lee, S., Kim, S., Hahn, Y.-B.: TiO_2 nanoparticles/nanotubes for efficient light harvesting in perovskite solar cells. Nanomaterials. 9, 326 (2019)

32. Khorasani, A., Marandi, M., Iraji zad, A., Taghavinia, N.: Application of combinative TiO_2 nanorods and nanoparticles layer as the electron transport film in highly efficient mixed halides perovskite solar cells. Electrochimica Acta. 297, 1071 (2019)

33. Cai, N., Moon, S.-J., Ha, L.C., Moehl, T., Humphry-Baker, R., Wang, P., Zakeeruddin, S.M., Gratzel, M.: An organic D-pi-A dye for record efficiency solid-state sensitized heterojunction solar cells. Nano Lett. 11, 1452 (2011)

34. Chang, J.A., Im, S.H., Lee, Y.H., Kim, H.-J., Lim, Ch.-S., Heo, J.H., Seok, S.L.: Panchromatic photon-harvesting by hole-conducting materials in inorganic-organic heterojunction sensitized-solar cell through the formation of nanostructured electron channels. Nano Lett. 12, 1863 (2012)

35. Liang, J., Wang, C., Wang, Y., Xu, Zh., Lu, Zh., Ma, Y., Zhu, H., Hu, Y., Xiao, Ch., Yi, X., Zhu, G., Lv, H., Ma, L., Chen, T., Tie, Z., Jin, Zh., Liu, J.: All-Inorganic Perovskite Solar Cells. J. Am. Chem. Soc. 138, 15289 (2016)

36. Hodes, G., Cahen, D.: All-solid-state, semiconductor-sensitized nanoporous solar cells. Acc. Chem. Res. 45, 705 (2013)

37. Liu, D., Kelly, T.L.: Perovskite solar cells with a planar heterojunction structure prepared using room-temperature solution processing techniques. Nature Photonics. 8, 133 (2014)

38. A. Kojima, K. Teshima, Y. Shirai, T. Miyasaka, Journal of American Chemical Society. 131, 6050 (2009)

39. Im, J.-H., Lee, C.-R., Lee, J.-W., Park, S.-W., Park, N.-G.: 6.5% efficient perovskite quantum-dot-sensitized solar cell. Nanoscale. 3, 4088 (2011)

40. Kim, S.-C., Kim, Y.-J.: An energy efficient priority-based MAC protocol for wireless sensor networks. International Conference on ICT Convergence (2012)

41. Lee, M.m., Teuscher, J., Miyasaka, T., Murakami, T.N., Snaith, H.J.: Efficient hybrid solar cells based on meso-superstructured organometal halide perovskites. Science. 338, 643 (2012)

42. Burschka, J., Pellet, N., Moon, S.-J., Humphry-Baker, R., Gao, P., Nazeeruddin, M.K., Grätzel, M.: Sequential deposition as a route to high-performance perovskite-sensitized solar cells. Nature. 499, 316 (2013)

43. Liu, M., Johnston, M.B., Snaith, H.J.: Efficient planar heterojunction perovskite solar cells by vapour deposition. Nature. 501, 395 (2013)

44. Yang, Zh., Zhang, Sh., Li, L., Chen, W.: Research progress on large-area provskite thin films and solar modules. Journal of Materiomics. 3, 231 (2017)

45. Qui, L., Ono, L.K., Qi, Y.: Advances and challenges to the commercialization of organic–inorganic halide perovskite solar cell technology. Materialy Today Energy. 7, 169 (2018)

46. Krull, U.J., Thompson, M.: Encyclopedia of Physical science and Technology: Analytical Chemistry, Encyclopedia of Physical, science and Technology: Analytical Chemistry, (3rd Ed Academic Press) (2001)

47. Tauc, J.: Optical properties and electronic structure of amorphous Ge and Si Materials Research Bulletin. 3, 37 (1968)

48. Wang, Y., Zhang, L., Deng, K., Chen, X., Zou, Z.: Low temperature synthesis and photocatalytic activity of rutile TiO_2 nanorode superstructures. J. Phys. Chem. C. 111, 2709 (2007)

49. Basore, P.A.: Numerical modeling of textured silicon solar cells using PC1D. IEEE Transactions on electron devices. 37, 337 (1990)

50. Lee, C., Efstathiadis, H., Raynolds, J.E., Haldar, P.: Two-dimensional computer modeling of single junction a-Si: H solar cells. In Photovoltaic Specialists Conference (PVSC) 34th IEEE (2009)

51. Hodes, G.: Perovskite-based solar cells. Applied physics Science. 342, 317 (2013)

52. Chen, Q.-Y., Huang, Y., Huang, P.-R., Ma, T., Cao, C., He, Y.: Electro negativity explanation on the efficiency-enhancing mechanism of the hybrid inorganic–organic perovskite ABX3 from first principles study. China Physics B. 25, 027104 (2015)

53. Xosrovashvili, G., Gorji, N.E.: Numerical analysis of TiO_2/Cu_2ZnSnS_4 nanostructured PV using SCAPS1D. Journal of Modern Optics, 60, 939 (2013)

54. Lin, P., Lin, L., Yu, J., Cheng, S., Lu, P., Zheng, Q.: Numerical Simulation of Cu2ZnSnS4 Based Solar Cells with In2S3 Buffer Layers by SCAPS-1D. Journal of Applied Science and Engineering. 17, 383 (2014)

55. Wu, H., Wang, L.-S.: A study of nickel monoxide (NiO),nickeldioxide(ONiO),and $Ni(O_2)Ni(O_2)$ com plex by anion photoelectron spectroscopy. The Journal of Chemical Physics. 107, 1621 (1998)

56. Madelung, O.: Semiconductors Data Handbook. (third ed. Springer), 1-247(2004)

57. Fonash, S.: Solar Cell Device Physics (second ed Academic Press) 1-381 (2010)

58. Stoumpos, C.C., Malliakas, C.D., Kanatzidis, M.G.: Semiconducting tin and lead iodide perovskites with organic cations: phase transitions, high mobilities, and near-infrared photoluminescent properties. Inorganic chemistry. 52, 9019 (2013)

59. Chen, D., Wang, Y., Lin, Z., Huang, J., Chen, X., Pan, D., Huang, F.: Growth strategy and physical properties of the high mobility p-type Cui crystal. Crystal Growth & Design. 10, 2057 (2010)

60. Yin, W.J., Shi, T.T., Yan, Y.F.: Unique properties of halide perovskites as possible origins of the superior solar cell performance. Advance Materials. 26, 4653 (2014)

61. Sze, S.M., Ng, K.K.: Physics of semiconductor devices, (Third edition), Wiley (2007)

62. Roiati, V., Colella, S., Lerario, G., Marco, L.D., Rizzo, A., Listorti, A.: Investigating charge dynamics in halide perovskite-sensitized mesostructured solar cells. Energy and Environmental Science. 6, 1889 (2014)

63. Marchioro, A., Teuscher, J., Friedrich, D., Kunst, M., van de Krol, R., Moehl, T., Grätzel, M., Moser, J.-E.: Unravelling the mechanism of photoinduced charge transfer processes in lead iodide perovskite solar cells. Nature Photonics. 8, 250 (2014)

64. Wang, X., Fang, Y., He, L., Wang, Q., Wu, T.: Influence of compact TiO_2 layer on the photovoltaic characteristics of the organometal halide perovskite-based solar cells. Materials Science in Semiconductor Processing. 27, 569 (2014)

65. Elumalai, N.K., Uddin, A.: Open circuit voltage of organics solar cells: An in-depth review. Energy Environmental. Science. 9, 391 (2016)

66. Li, Ch., Lv, L., Qin, L., Zhu, L. Teng, F., Lou, Zh., Deng, Zh., Hu, Y., Cui, Q., Hou, Y.: Investigation on the Overshoot of Transient Open-Circuit Voltage in Methylammonium Lead Iodide Perovskite Solar Cells. Materials. 11, (2018)

67. Poddar, N.P., Mukherjee, S.K.: Characterization of TiO2thin films deposited by using dc magnetron sputtering. Carbon–Sci. Tech. 8, 1 (2016)

68. Singh, P., Kaur, D.: Room temperature growth of nanocrystalline anatase TiO_2 thin films by dc magnetron sputtering. Physica B: Condensed Matter. 405, 1258 (2010)

69. Nair, P.B., Justin victor, V.B., Daniel, G.P., Joy, K., Ramakrishnan, V., Thomas, P.V.: Effect of RF power and sputtering pressure on the structural and optical properties of TiO_2 thin films prepared by RF magnetron sputtering. Applied Surface Science. 257, 10869 (2011)

Figures

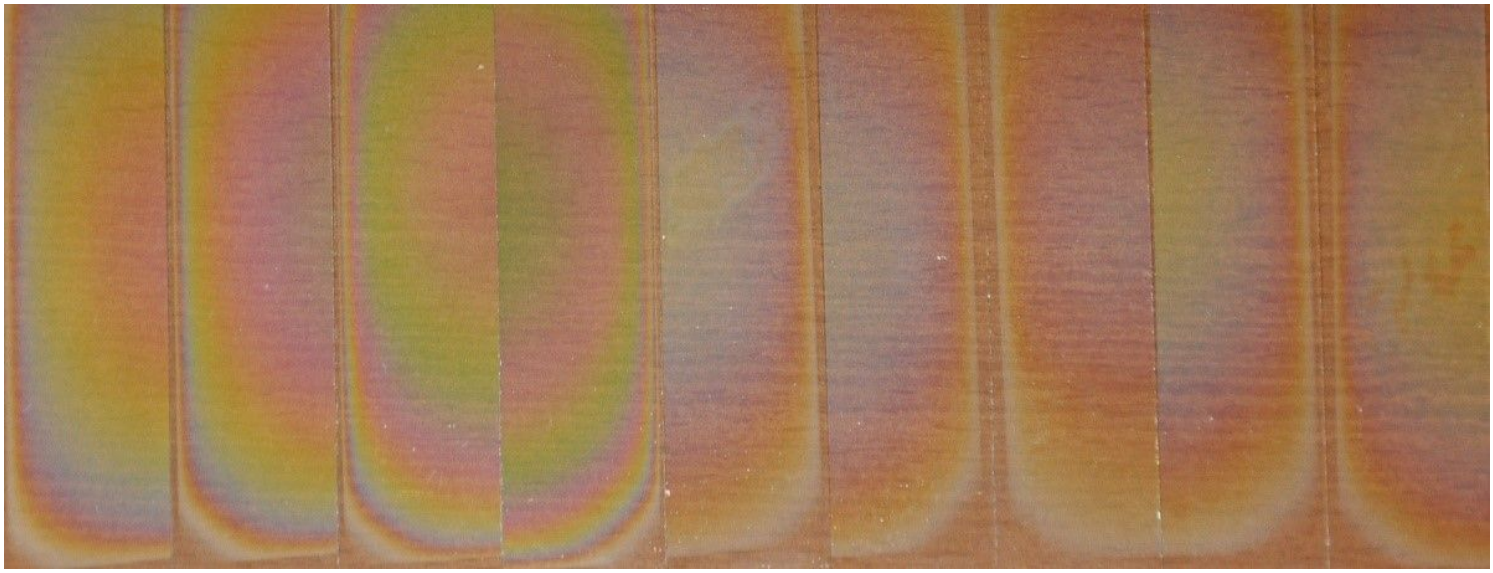

Figure 1

Tio2 laboratory samples made in different laboratory conditions.

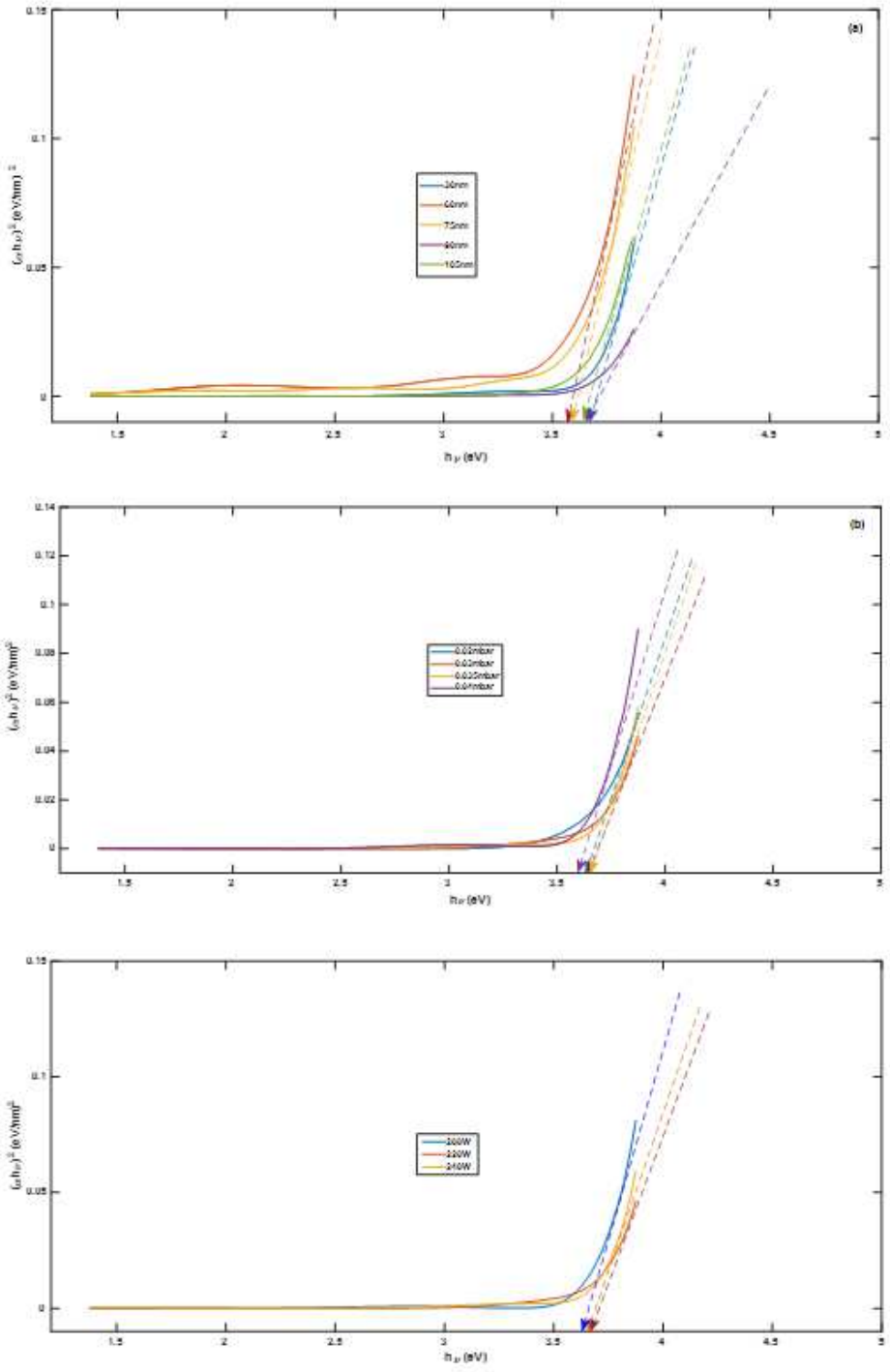

Figure 2

Tauc's plot for the thin film prepared TiO2 a) different thicknesses, b) under different pressures, c) Different powers

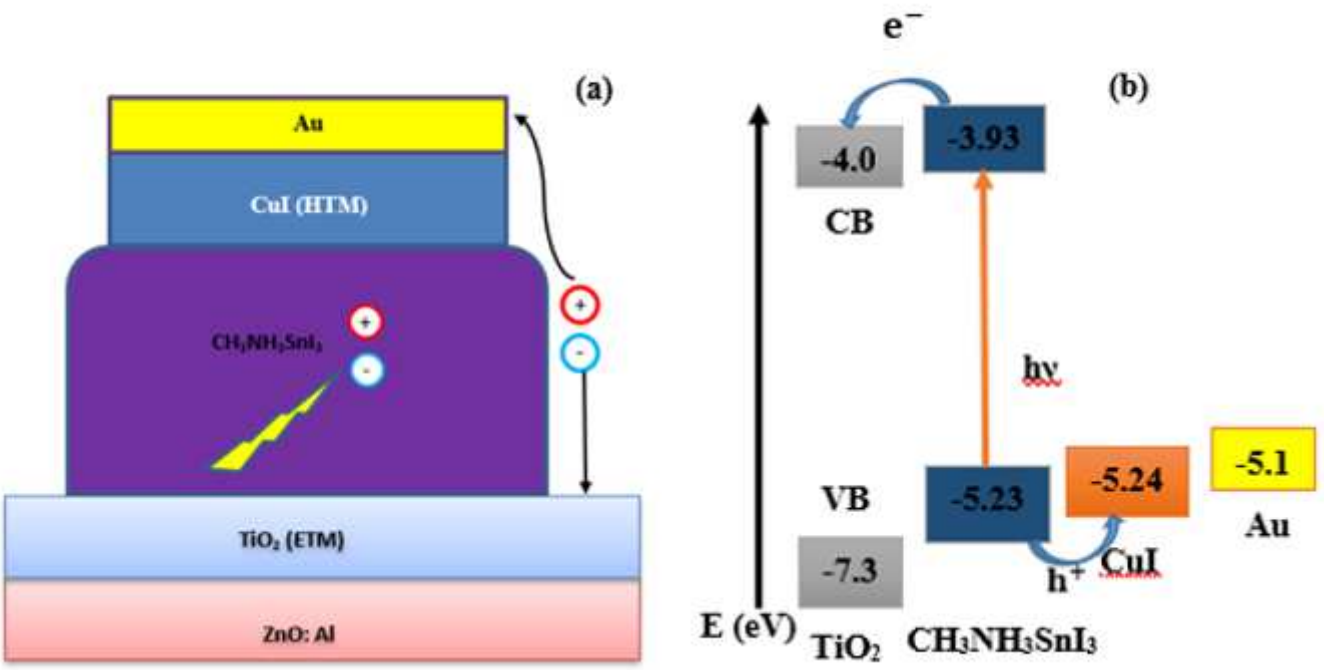

Figure 3

a) Schematic structure and b) perovskite solar cell energy diagram CH3NH3SnI3

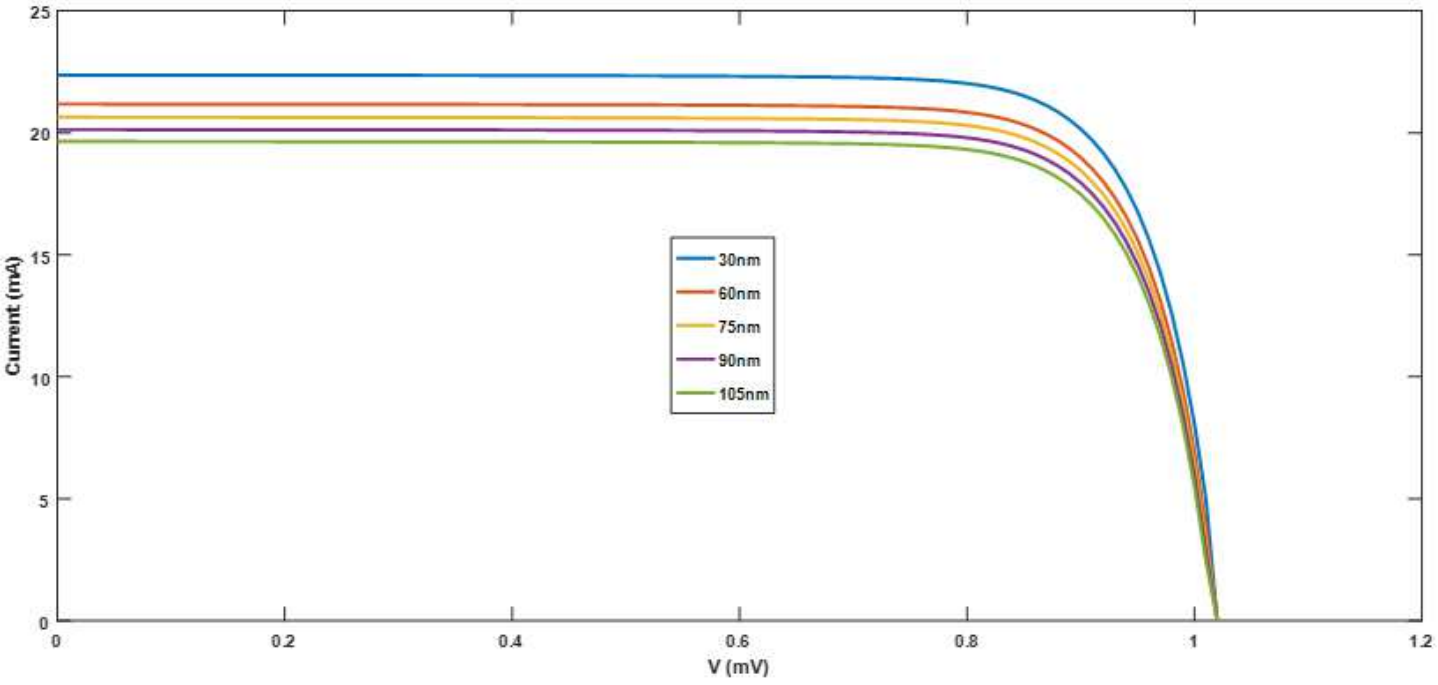

Figure 4

I-V curve perovskite solar cell for different thicknesses.

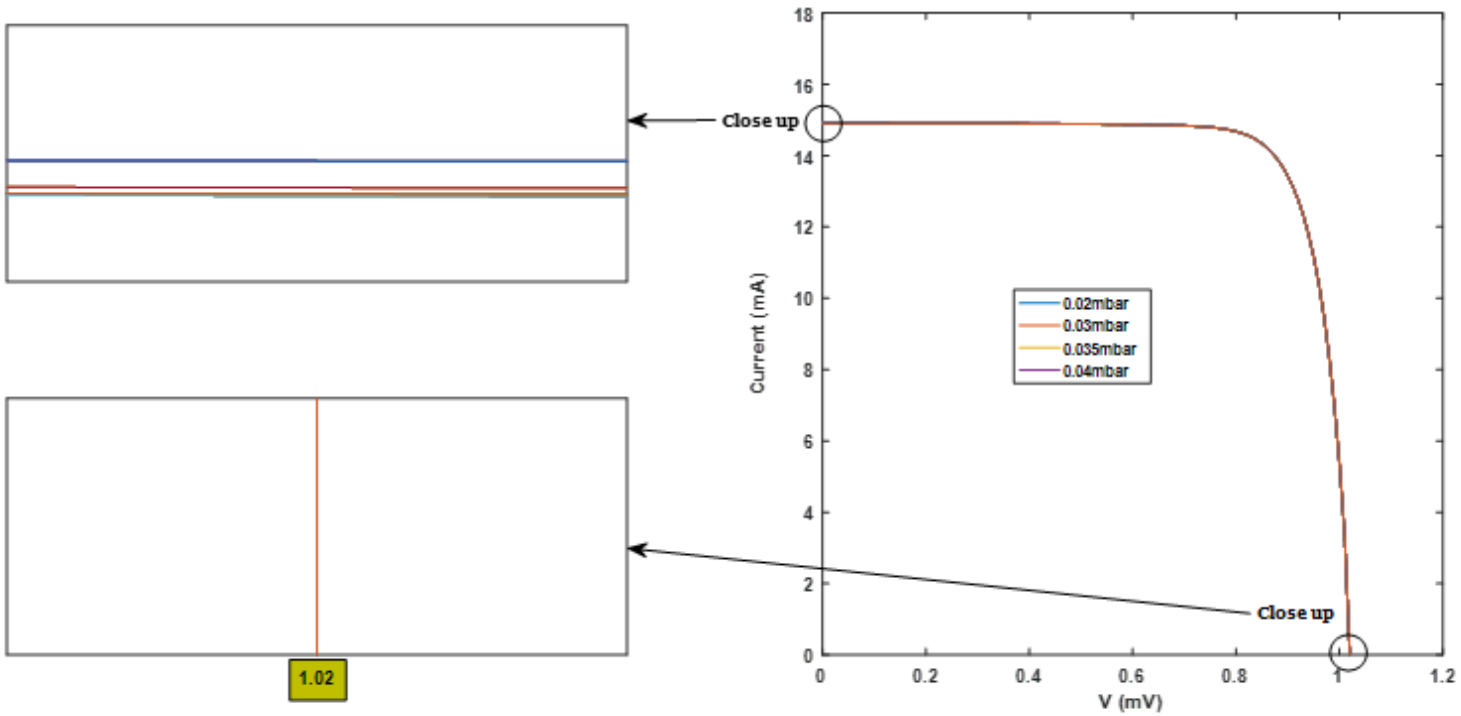

Figure 5

I-V curve perovskite solar cell for different pressures.

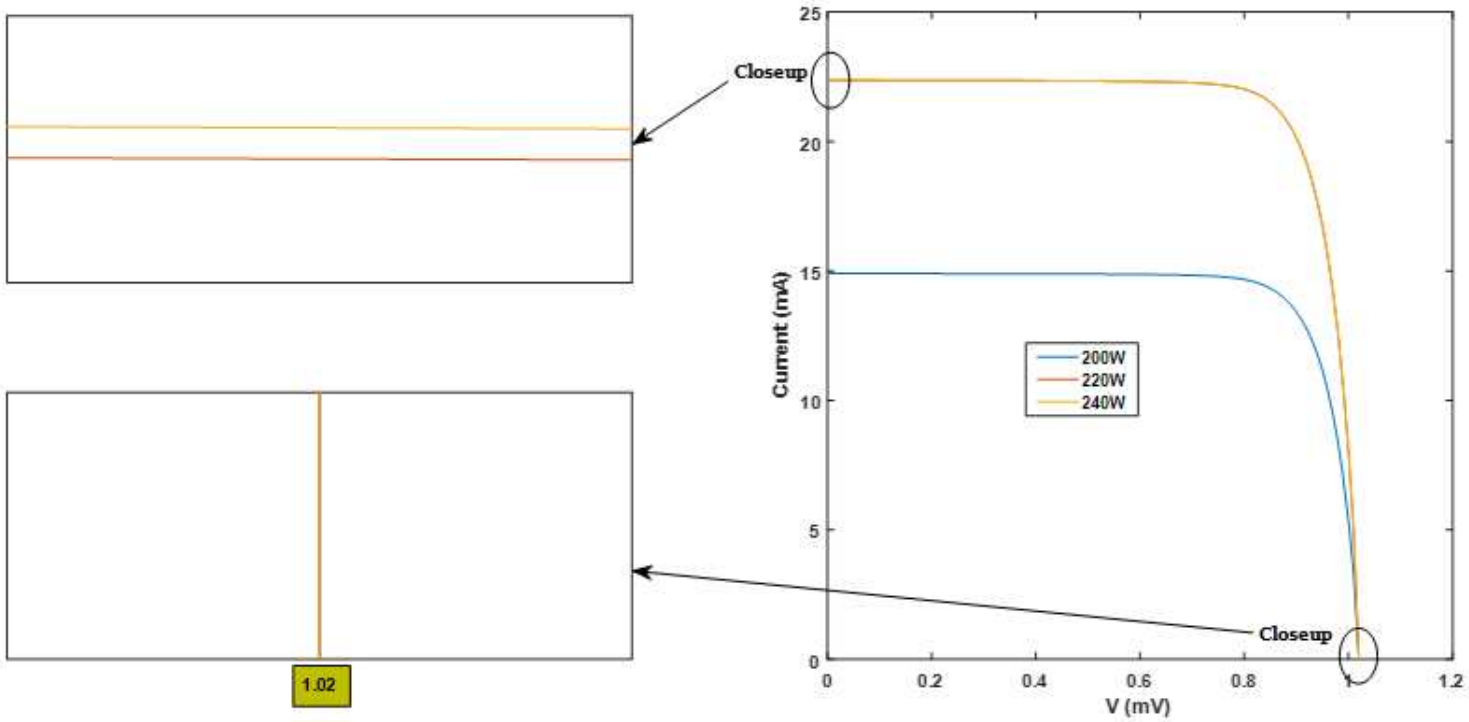

Figure 6

I-V curve perovskite solar cell for different powers.

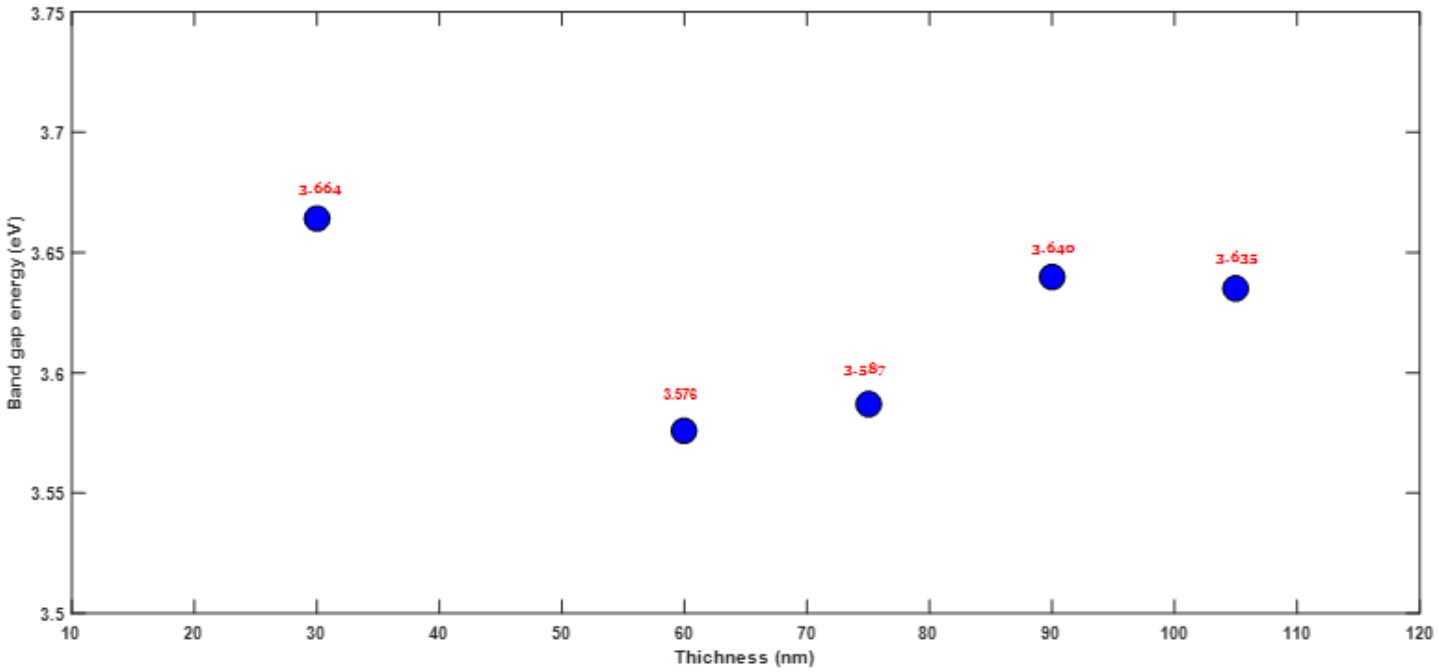

Figure 7

TiO2 compact layer bands gap energy as a function of the layer's thickness.

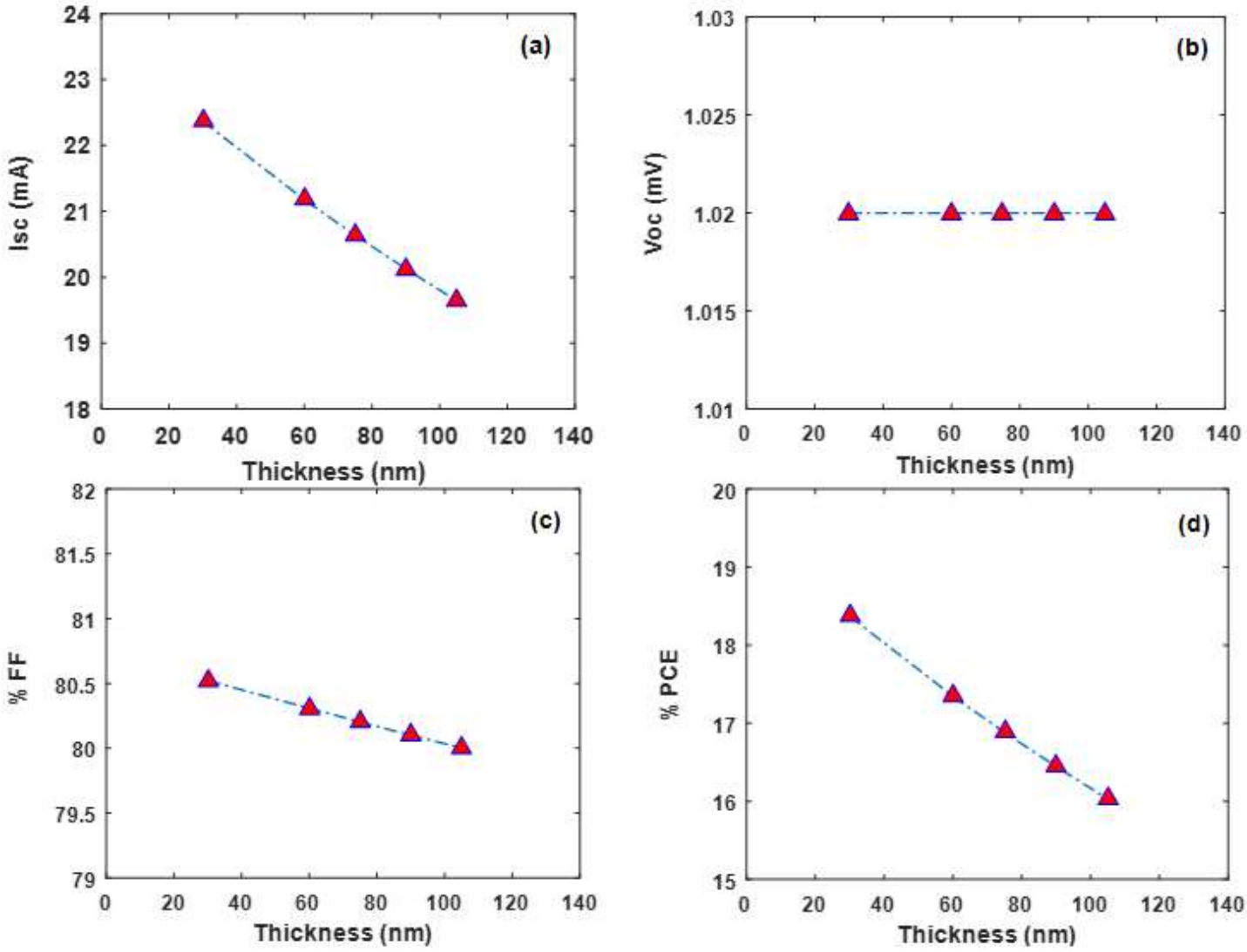

Figure 8

Compact layer (CL) thickness-dependent variation in (a) Is c, (b) Vo c, (c) % FF, and (d) % PCE.

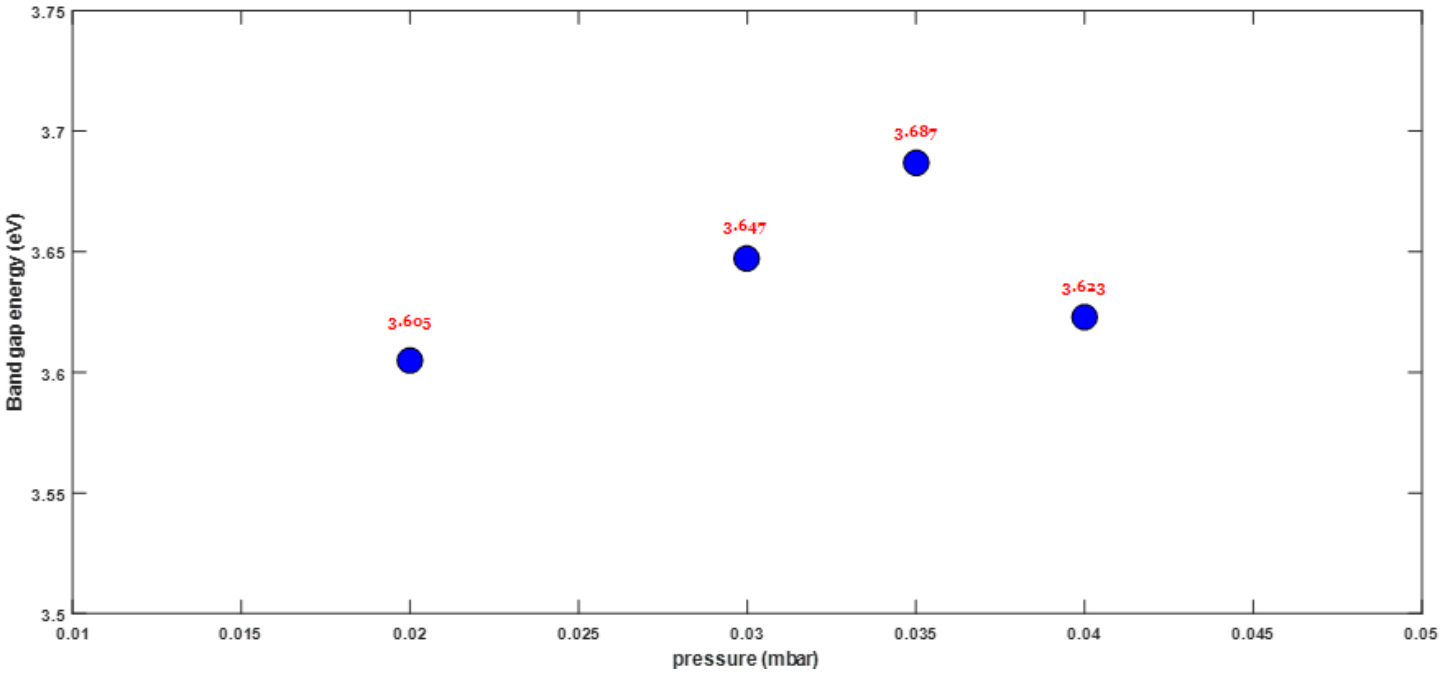

Figure 9

TiO2 compact layer bands gap energy as a function of chamber's pressure.

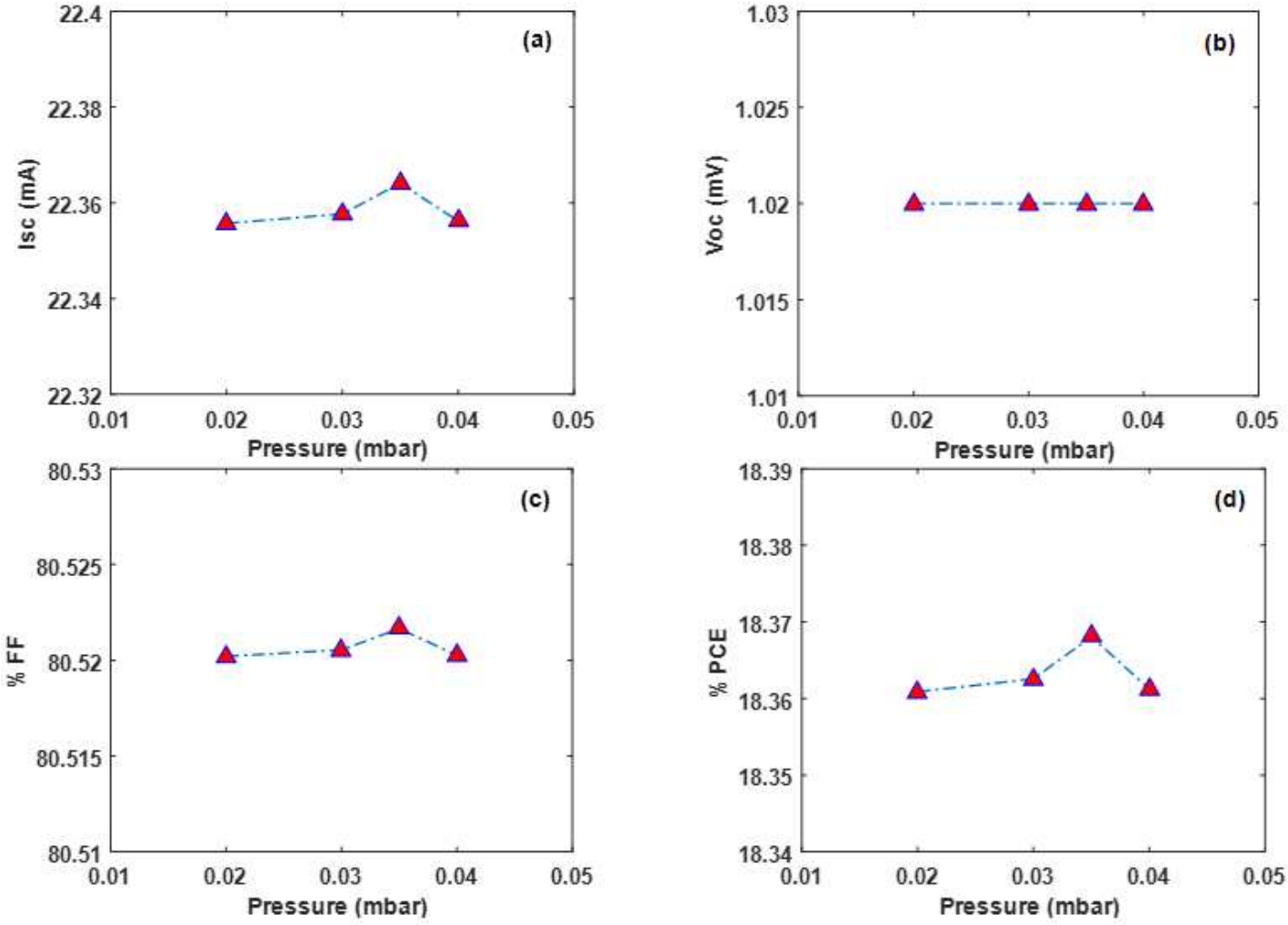

Figure 10

Compact layer (CL) pressure-dependent variation in a) Isc, b) Voc, c) % FF, and d) % PCE

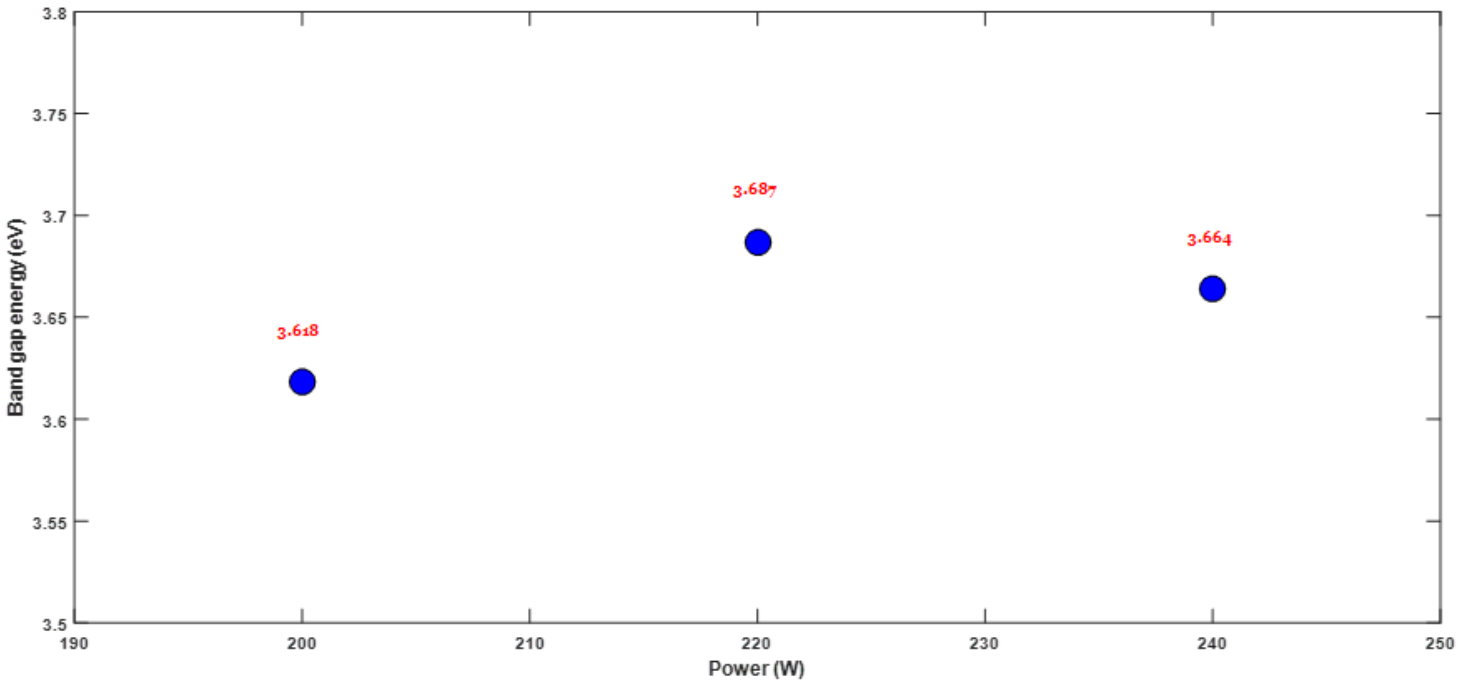

Figure 11

TiO2 compact layer bands gap energy as a function of deposition power.

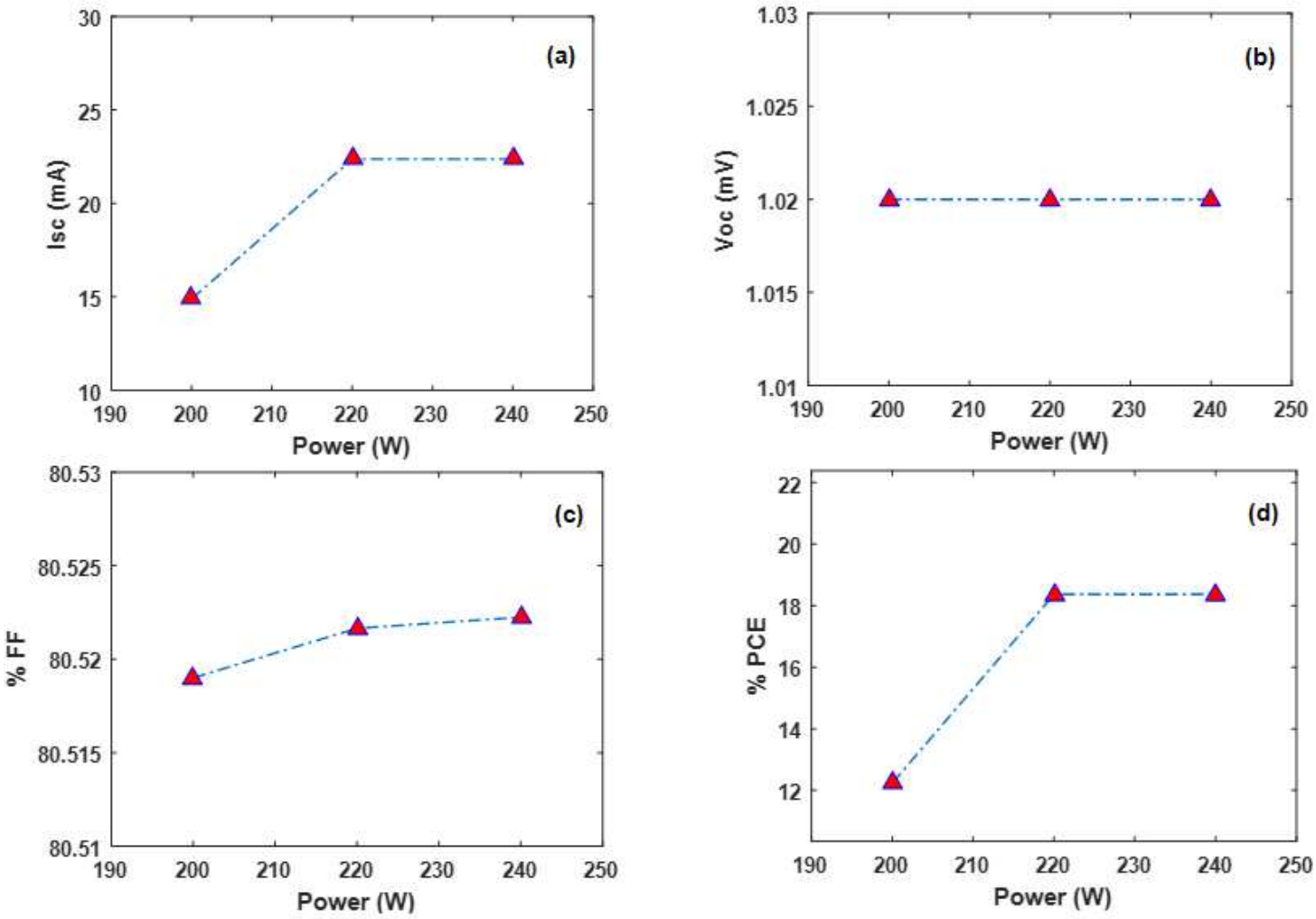

Figure 12

compact layer (CL) Power-dependent variation in a) Isc, b) Voc, c) % FF, and d) % PCE